Macromolecules

ARTICLE

pubs.acs.org/Macromolecules

Unified Description of the Viscoelastic and Dielectric Global Chain Motion in Terms of the Tube Theory

T. Glomann,[†] G. J. Schneider,[*,‡] A. R. Brás,[†] W. Pyckhout-Hintzen,[†] A. Wischnewski,[†] R. Zorn,[†] J. Allgaier,[†] and D. Richter[†]

[†]Jülich Centre for Neutron Science & Institute for Complex Systems, Forschungszentrum Jülich, 52425 Jülich, Germany

[‡]Jülich Centre for Neutron Science, Forschungszentrum Jülich, Outstation at FRM 2, Lichtenbergstrasse 1, 85747 Garching, Germany

ABSTRACT: We present a new approach to a unified description of the dielectric end-to-end vector and the viscoelastic stress relaxation of entangled homopolymer melts in terms of the tube model. The comparison and quantitative analysis of carefully recorded viscoelastic and dielectric relaxation spectra evidence that the dielectric mode distribution is completely determined by reptation and contour length fluctuations and thus is insensitive to the CR process within experimental accuracy. We show that a joint analysis of viscoelastic and dielectric experiments allows an accurate characterization of pure single chain dynamics. The general validity of our approach is demonstrated on monodisperse polyisoprene (PI) for a wide range of different molecular weights and on poly(butylene oxide) (PBO).

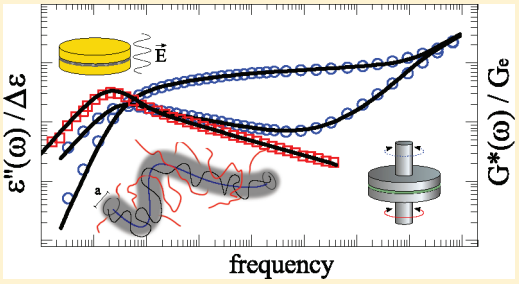

INTRODUCTION

Broadband measurement techniques are widely used for the investigation of the numerous relaxation phenomena occurring in linear flexible polymer chains. Concerning the large scale dynamics of e.g. polyisoprene, dielectric and mechanical spectroscopy detect both the same global chain motion.[1] Yet over a wide spectral range the microscopic chain dynamics are quite differently reflected, a unique feature which can be used to scrutinize the current tube model concepts.

Above the critical molecular weight M_c polymer chains mutually interpenetrate and entangle, thereby severely restricting the possible chain motions to a laterally confined tubelike region that follows the coarse-grained chain contour, the primitive path. In the ingenious reptation theory, originally proposed by de Gennes[2] and later generalized by Doi and Edwards,[3] this confined motion was modeled in a mean-field approach as a one-dimensional diffusion along the tube profile known as reptation.

Although the tube model is able to predict the essential part of entanglement dynamics, two refinements have to be included to accurately model the viscoelastic properties of real (finite length) polymer melts: (i) Near the chain ends where the motion is less confined the thermal fluctuations of the chain length lead to a gradual erosion of the confining tube starting from both ends.[4,5] This single-chain correction, known as contour length fluctuations (CLF), shortens the longest relaxation time needed for the chain to disentangle, i.e. escaping the tube, and induces characteristic power law behavior in the spectrum on shorter time scales. (ii) Since all chains in the melt are equally moving, the motion of the confining virtual tube has to be considered as well. Viscoelastic experiments reveal that the associated lateral softening of the tube, described as constraint release (CR), similarly accelerates the terminal relaxation. It is an intrinsic many-body effect and therefore difficult to assess quantitatively neither by theory nor by experiments.[4]

As has been extensively reported in the literature the experimentally measured frequency-dependent normalized viscoelastic and dielectric relaxation functions of entangled chains do not superimpose on each other.[6−9] The viscoelastic relaxation spectrum is much broader than the corresponding dielectric spectrum, and also the respective longest relaxation times do not coincide. These experimental observations evidence the fundamental differences in the involved correlation functions. While the viscoelastic stress relaxation reflects the isochronal orientational anisotropy of bond vectors $S(t)$ along the chain, the dielectric normal mode relaxation directly reveals the end-to-end vector correlation function $\langle \vec{R}(t)\vec{R}(0)\rangle$ of the chain.[10]

A comprehensive quantitative molecular theory for the viscoelastic relaxation of entangled linear chains was developed by Likhtman and McLeish (LM);[4] however, a comparable microscopic interpretation of the dielectric normal mode spectrum is missing.[1,7,8,10−15] Moreover, in the case of polyisoprene, there is even disagreement about the spectral shape of the normal mode and its dependence on the molecular weight.[1,7,8,10,13−16]

All recent publications on the dielectric normal mode of highly entangled PI eventually confirm the existence of two distinct power law regions on the high-frequency side of the peak in the dielectric loss $\varepsilon''(\omega)$ with the characteristic slopes of $-1/2$ and $-1/4$ as expected by the tube theory.[1,13−15] Nonetheless, any attempts to describe the molecular origin of the spectral shape in terms of reptation, CLF, and CR are either missing completely, reported to fail, or give an unsatisfactory description over the full frequency range.[1,8,10,13−15]

Received: March 24, 2011
Revised: August 12, 2011
Published: August 29, 2011

On the basis of the particular features of the involved correlation functions, we present a new straightforward approach to a quantitative molecular picture of the dielectric global chain relaxation in terms of the well-known tube theory. We show that the precise Likhtman−McLeish solution to the tube occupation function $\mu(t)$, i.e., the self-consistent combination of reptation and contour length fluctuations, can sufficiently well describe all the features of the dielectric end-to-end vector relaxation.

Our experimental findings on PI and PBO homopolymer melts further evidence that the dielectric end-to-end vector relaxation is apparently quite insensitive to the thermal constraint-release motion of the tube forming chains. Earlier works on PI/PB and PI/PI blends[1,9,17−20] also report the CR insensitivity of the dielectric mode distribution and thus support our findings for homopolymer melts. From this fact we draw the conclusion that broadband dielectric measurements allow the direct observation of the single chain motion isolated from the tube motion.

The general validity of our approach is demonstrated by the quantitative analysis of viscoelastic and dielectric experiments on monodisperse polyisoprene (PI) for a wide range of molecular weights and on the chemically different poly(butylene oxide) (PBO).

THEORETICAL BACKGROUND

In the tube model the correlation functions involved in viscoelastic and dielectric relaxation can be formulated using a coarse-grained picture where the whole chain is divided into N Gaussian submolecules and the bond vector $\vec{u}(n,t)$ denotes the end-to-end vector of the nth submolecule at time t.[1,4] Each of the submolecules with size b and friction coefficient ζ is connected by entropic springs with force constant $\kappa = 3k_BT/b^2$, where k_B is the Boltzmann constant and T the temperature. The confining tube itself is modeled as a Gaussian random walk with an effective tube diameter a. It is composed of $Z = N/N_e = Nb^2/a^2$ entanglement segments, where each segment has the molar entanglement mass $M_e = M/Z$.[4] The unconfined chain sections inside these segments relax via fast Rouse relaxation on the time scale $\tau_e = N_e{}^2\zeta b^2/(3\pi^2 k_BT)$.[4] In the case of pure reptation the time scale for the global chain relaxation is then given by the reptation time $\tau_d = 3Z^3\tau_e$.[4]

Viscoelastic Relaxation. The linear viscoelastic relaxation modulus $G(t)$ contains all viscoelastic properties of the material. It is obtained by measuring the decay of the generated stress within the sample after a small step strain γ at time $t = 0$. This $G(t)$ can be expressed as sum over the orientational correlation function $S(n,t)$, which describes the isochronal orientational anisotropy of the nth submolecule of size b:[1,8]

$$S(n,t) = \frac{\langle u_i(n,t)u_j(n,t)\rangle}{b^2} \tag{1}$$

where the indices i, j denote the components of the bond vector $\vec{u}(n,t)$ in the shear and shear gradient directions at time t.

The experimentally easily accessible viscoelastic storage $G'(\omega)$ and loss moduli $G''(\omega)$ are given by the real and imaginary parts of the Fourier transformation of $G(t)$.[21]

Dielectric Relaxation. In analogy to the viscoelastic case, the dielectric relaxation detects the macroscopic response of the material subject to an external perturbance by applying a small electric field $\vec{E}(t)$. The time dependence of the macroscopic polarization $\vec{P}(t)$ of the system contains the dynamic features of the chain motion.[1] The polarization originates from the orientation of molecular dipoles along the direction of the external electric field $\vec{E}(t)$.

Following the classification by Stockmayer,[22] only the so-called type-A polymers, which have a permanent dipole moment $\vec{\mu}_i$ attached in parallel to the backbone of the monomeric units, are susceptible for the slow dielectric or global chain relaxation. The macroscopic polarization $\vec{P}(t)$ is given by the sum over all molecular dipoles or coarse grained bond vectors $\vec{u}(n,t)$ per unit volume:

$$\vec{P}(t) = \sum_i \vec{\mu_i}(t) = \sum_n \vec{u}(n,t) \tag{2}$$

In homogeneous and isotropic systems, the autocorrelation of $\vec{P}(t)$ specifies all the relevant dielectric features of the chain relaxation[1] and defines the normalized dielectric relaxation function $\phi(t)$:

$$\phi(t) = \frac{\langle \vec{P}(t)\cdot\vec{P}(0)\rangle}{\langle P^2\rangle} \tag{3}$$

For PI the cross-correlations between dipoles of different chains can be neglected;[1] therefore, $\phi(t)$ is determined by the local orientational autocorrelations $C(n,t,n')$ between different segments n and n' within the same chain:[1]

$$C(n,t,n') = \frac{\langle \vec{u}(n,t)\cdot\vec{u}(n',0)\rangle}{\langle u^2\rangle} \tag{4}$$

Likhtman−McLeish Theory. The equations of motions given by the generalized tube model for the viscoelastic relaxation of linear chains cannot be solved analytically.[4,10] The Likhtman−McLeish theory provides a sufficiently accurate mathematical approximation by a self-consistent combination of reptation, contour length fluctuations, constraint release, and longitudinal stress relaxation.[4] Here, we summarize the essential results and refer to the original work[4] for the complete definition of the formulas.

By combining analytical treatment with stochastic simulations, the theory derives an expression for the tube occupation function $\mu(t)$, i.e., the solution to the single chain problem of reptation and CLF, where all parameters are defined by the microscopic chain properties from the tube model. The expression for the single chain solution $\mu(t)$ is the sum of two parts:

$$\mu(t) = G_f(Z)\sum_{p=1,\,\mathrm{odd}}^{p^*}\frac{8}{p^2\pi^2}\exp\left(-\frac{p^2t}{\tau_{df}(Z)}\right) + \int_{\varepsilon^*}^{\infty}\frac{0.306}{Z\tau_e{}^{1/4}\varepsilon^{5/4}}\exp(-\varepsilon t)\,\mathrm{d}\varepsilon \tag{5}$$

The reptation-dominated first part expresses the late time relaxation which is formally identical to a renormalized pure reptation spectrum[3] where the rescaled modulus $G_f(Z)$ and reptation time $\tau_{df}(Z)$ are functions of the number of entanglements Z. The solution for the CLF dominated early time relaxation is given by the second part in eq 5 as an analytical expression to describe the enhanced relaxation near the chain ends. The transition between both regimes happens exponentially abruptly.[4]

The effects of CLF on the chain relaxation can easily be illustrated by plotting the imaginary part $\mu''(\omega)$ of the Fourier

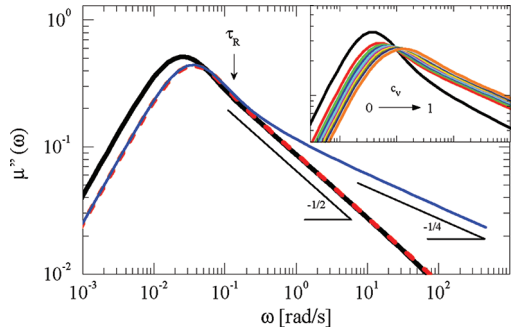

Figure 1. Illustration of the two effects of CLF on the pure reptation process (black line) for highly entangled chains ($Z = 100$). At long times, CLF renormalizes the reptation peak (red dashed line) and at shorter times the slope changes to $-1/4$ (blue line). The inset shows the effect of CR on reptation including CLF for increasing values of c_ν in 10 steps from 0 to 1.

Table 1. Sample Labels, Molecular Weights M_w, and Polydispersities M_w/M_n

polymer	M_w [kg/mol]	M_w/M_n
PI-45	45	1.04
PI-66	66	1.03
PI-80	80	1.04
PI-140	140	1.04
PI-224	224	1.04
PI-314	314	1.04
PBO-100	104	1.06

transformation of eq 5 as displayed in Figure 1 for the instructive case of a highly entangled chain ($Z = 100$). For long times ($t > \tau_R$) the contour length fluctuations act simply like a renormalization to the pure reptation (black line) by accelerating the reptation time (peak shifts to higher frequencies) and decreasing the modulus height.[4] For shorter times ($t < \tau_R$) the fluctuations change the power law spectrum from the $-1/2$ slope (pure reptation) to a characteristic $-1/4$ slope (reptation + CLF), resulting in a distinct kink in the loss modulus of the full single chain relaxation (blue line).

In this theory the problem of CR, the time evolution of the tube motion $R(t)$, is assumed to be independent of the single chain dynamics $\mu(t)$ and follows the self-consistent solution of Colby and Rubinstein.[23] The moving tube $R(t,c_\nu)$ is described as a relaxing Rouse chain with tube segment mobilities m_i distributed randomly according to a probability distribution $P(\varepsilon)$ calculated from the single chain solution $\mu(t)$:[4]

$$R(t, c_\nu) = \left\langle \int_0^\varepsilon \mathrm{d}\varepsilon \frac{\mathrm{d}M}{\mathrm{d}\varepsilon} \exp(-\varepsilon c_\nu t) \right\rangle \tag{6}$$

The brackets indicate the statistical average over the distribution of mobilities. This function introduces an additional parameter c_ν that parametrizes the strength of the tube relaxation as illustrated in the inset of Figure 1. The colored lines show the influence of gradually increasing values of c_ν ranging from 0 (no CR, black) to 1.0 (effective jump of the tube over a distance of its diameter, orange) on the single chain spectrum for $Z = 100$ (reptation + CLF, blue). The CR motion first flattens the peak for small c_ν and then shifts the peak to higher frequencies for $c_\nu > 0.3$.[4]

The corresponding longest relaxation time of the Rouse tube scales as $\tau_{CR} \sim \tau_d Z^2 \sim Z^5$ and is thus much slower than the reptation process of the relaxing probe chain.[4]

Furthermore, the LM theory states that only 4/5 of the total stored stress in the tube relaxes via the above-mentioned relaxation mechanisms. The remaining 1/5 relaxes via the so-called longitudinal stress relaxation which basically describes redistribution of monomers along the tube.[4,24]

The full expression for the description of the viscoelastic relaxation modulus $G(t)$ over the full time scale including τ_e is then given by

$$G(t) = G_e \left[\frac{4}{5}\mu(t)R(t, c_\nu) + \frac{1}{5Z}\sum_{p=1}^{Z-1} \exp\left(-\frac{p^2 t}{\tau_R}\right) + \frac{1}{Z}\sum_{p=Z}^{N} \exp\left(-\frac{2p^2 t}{\tau_R}\right) \right] \tag{7}$$

where the first term uses the above-mentioned independence assumption of single- and many-chain dynamics to formulate their competition as a product of both functions. The second term describes the just mentioned longitudinal stress relaxation, and the third term gives an approximation for the fast Rouse motion inside the tube.

The prefactor G_e defines the finite entanglement modulus $G_e = \rho RT/M_e$ as the stored stress σ in the tube at the time scale where the entanglement segments have relaxed via internal Rouse motion ($t > \tau_e$).

Model for the Dielectric Normal Mode. Motivated by experimental findings, we propose a straightforward approach to a new quantitative description of the dielectric normal mode relaxation spectrum based only on the molecular tube model parameters τ_e and Z.

In the case of an immobile tube, i.e., absence of CR motion, the correlation functions eq 1 and eq 4 predict the general coincidence of the dielectric and viscoelastic relaxation functions $\phi(t) = \mu(t)$.[1] Since experiments on dilute probe chains in low and high molecular weight matrices revealed that the dielectric mode spectrum is apparently insensitive to CR,[1,18,19] we assume that the dielectric relaxation function $\phi(t)$ for entangled linear chains may entirely be given by the LM single chain solution $\mu(t)$ in eq 5. We then propose a constitutive equation for the dielectric permittivity $\varepsilon(t)$:

$$\varepsilon(t) = \varepsilon_s - \Delta\varepsilon\mu(t) \tag{8}$$

The static dielectric constant ε_s is the limiting permittivity at low frequencies, and $\Delta\varepsilon$ denotes the dielectric relaxation strength.

Using eqs 7 and 8 allows us to obtain a joint description of both viscoelastic and dielectric data sets with the same set of molecular parameters τ_e and Z. In the present study we intend to show our proposed model and verify the assumption made for deducing eq 8 by comparing the imaginary part of the Fourier transform of $\varepsilon(t)$ to our measured dielectric spectra.

EXPERIMENTAL SECTION

In order to perform the aforementioned test, we carefully recorded viscoelastic and dielectric data of monodisperse polyisoprene samples over a wide range of molecular weights in the entanglement regime under identical conditions. Moreover, our analysis can also be used to test the universality of entanglement dynamics.[4] We therefore recorded data for another type-A polymer, poly(butylene oxide).

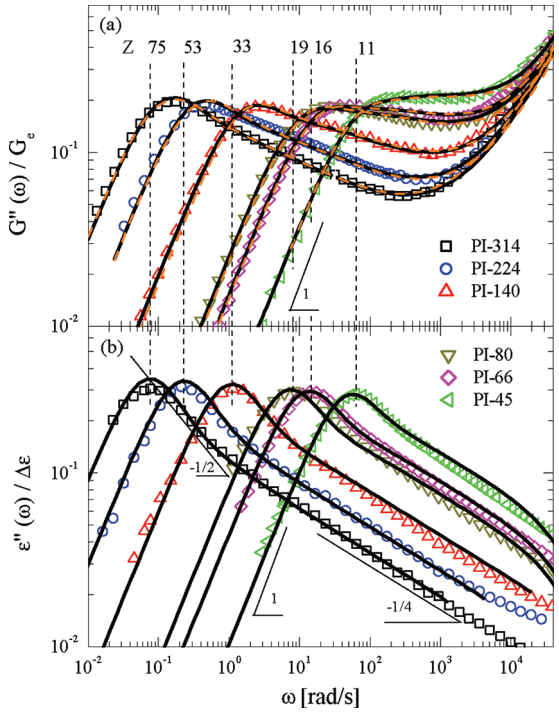

Figure 2. (a) Normalized loss modulus $G''(\omega)/G_e$ and (b) normalized dielectric loss $\varepsilon''(\omega)/\Delta\varepsilon$ at the reference temperature $T_0 = 25$ °C. The solid lines represent the joint description of both data sets with eqs 7 and 8 (see text). The thin dashed lines indicate the shift in the peak positions.

Samples. The experiments were performed on model systems comprising nearly monodisperse ($M_w/M_n \leq 1.05$) polyisoprene (PI) and poly(butylene oxide) (PBO) homopolymers. All polyisoprene samples were synthesized at the Forschungszentrum Jülich by anionic polymerization following well-established standard procedures.[25] The microstructure of the PI-66 sample was analyzed by the ^{1}H NMR technique and yielded a high content of cis-1,4 units of around 70%. We expect a similar microstructure for all other polyisoprenes as they were polymerized under the same conditions. The synthesis of the PBO polymer is described in detail in ref 26. The molecular weights M_w of all samples were characterized by static light scattering, and their molecular weight distribution M_w/M_n was determined by GPC measurements. The sample details are summarized in Table 1.

Rheology. All rheological measurements were performed on an ARES (TA Instruments) rheometer in the temperature range of −50 to 55 °C at frequencies between 100 and 0.1 rad/s at a fixed strain amplitude of 1% (linear regime). The parallel plate geometry with 8 mm plates was used, and the sample thickness was typically around 1 mm. The spectra were shifted according to the WLF time−temperature superposition principle[27] to the reference temperature $T_0 = 25$ °C. The temperature stability was better than 0.1 °C.

Broadband Dielectric Spectroscopy. Broadband dielectric measurements were conducted using a high-resolution Alpha dielectric analyzer by Novocontrol GmbH using gold-plated electrodes with a diameter of 20 mm. Glass fiber spacers ensured a constant sample thickness of 50 μm. Excluding PI-66, all samples were measured at the reference temperature of rheology with a temperature stability better than 0.1 °C. The PI-66 sample was measured at 27 °C but shifted to the same reference temperature according to the WLF equation using the parameters $c_1 = 4.8$ and $c_2 = 134.4$.

The conductivity contributions at low frequencies were carefully subtracted and the obtained spectra were normalized to the dielectric relaxation strength $\Delta\varepsilon$ by numerical integration over $\varepsilon''(\omega)$: $\Delta\varepsilon = 2/\pi\int\varepsilon''(\omega)\,\mathrm{d}\ln\omega$. We did not subtract the contribution from the alpha-process (segmental correlations) since its influence on the spectrum is negligible in the frequency range of the normal mode relaxation.

Table 2. Summary of All Fit Parameters Obtained from Modeling the Viscoelastic Polyisoprene Data to the LM Theory (eq 7)

sample	Z	c_ν	G_e (10^5 Pa)	τ_e (10^{-5} s)	M_e (kg/mol)
PI-45	11.0	0.30	4.8	1.4	4.1
PI-66	16.0	0.42	4.8	1.6	4.1
PI-80	19.4	0.52	5.8	1.4	4.1
PI-140	31.0	0.30	5.5	1.6	4.5
PI-224	56.8	0.60	5.4	1.5	3.9
PI-314	76.5	0.69	5.1	1.8	4.1

Data Analysis. We used our own implementation of the LM theory which, in contrast to e.g. "Reptate",[28] allows us to evaluate the different contributions in eq 7 individually, and the empirical CR parameter c_ν can continuously be varied. We allowed independent fitting of the parameters Z and G_e which are in principle coupled via their relation to M_e. The best fit to the data points was obtained by using the Nelder−Mead simplex minimization algorithm.[29]

RESULTS

At first we focus on the polyisoprene samples. Figure 2 displays the normalized viscoelastic (a) and dielectric (b) response for the different molecular weights at the same reference temperature. For the sake of clarity, only the loss parts $G''(\omega)$ and $\varepsilon''(\omega)$ of the measured spectra are shown.

In the frequency range from 10^{-2} to about 10^3 rad/s both experimental techniques equally detect the same essential features of the global chain relaxation: The terminal flow regime at low frequencies ω is characterized by a Debye-like power law dependence ω^1 in the respective loss parts of both spectra and the longest relaxation times, represented by the position of the reptation peaks, clearly show a very similar molecular weight dependency.

However, when both spectra are directly compared with respect to the peak positions (indicated by the thin dashed lines), the peak shapes and the observed slopes at higher frequencies, it becomes immediately obvious that the chain relaxation spectrum is differently reflected in the viscoelastic and dielectric experiment. For all molecular weights the peak widths in the dielectric spectra (Figure 2b) are all similarly narrow and show two distinctly different slopes on the high frequency part of the peak as indicated by the thin lines. While the slope in the vicinity of the peak is consistent with the expectation from pure reptation (−1/2), the slope at higher frequencies well conforms to the characteristic value for CLF of about −1/4. On the contrary, the peak widths in the viscoelastic spectra (Figure 2a) clearly broaden with decreasing molecular weight, and for very high frequencies the loss modulus $G''(\omega)$ increases strongly independent of molecular weight.

The solid lines represent the best fits following our joint description of dielectric and viscoelastic data which was performed by the following procedure: At first, only the viscoelastic data $G'(\omega)$ and $G''(\omega)$ were simultaneously fitted to the LM theory given by eq 7 whereupon all parameters (τ_e, G_e, Z, c_ν) were freely varied. Fitting the data separately for each molecular weight sample yields on average $\tau_e = (1.6 \pm 0.3) \times 10^{-5}$ s, $G_e = (0.53 \pm 0.05) \times 10^5$ Pa, and the values for c_ν vary unsystematically between 0.3 and 0.7. On average, the fitted number of entanglements Z correspond to an entanglement molecular weight $M_e = 4.1 \pm 0.3$ kg/mol.

dx.doi.org/10.1021/ma200674z |*Macromolecules* 2011, 44, 7430–7437

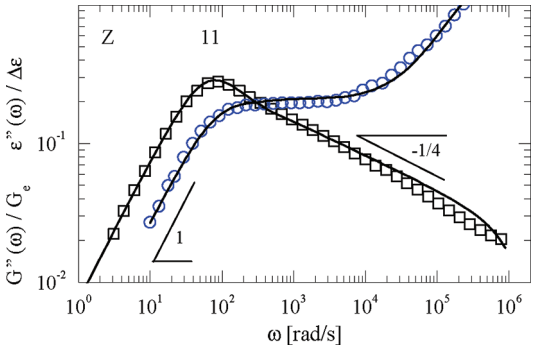

Figure 3. Comparison of measured viscoelastic (circles) and dielectric (squares) losses of PBO with a molecular weight M_w = 86 kg/mol. The lines show the joint theory descriptions with eqs 7 and 8.

Table 3. Summary of All Fit Parameters Obtained from the Joint Description of the Viscoelastic and Dielectric Data

sample	Z	c_ν	G_e (10^5 Pa)	τ_e (10^{-5} s)	M_e (kg/mol)
PI-45	10.8	0.35	4.8	1.6	4.2
PI-66	16.0	0.41	4.7	1.6	4.1
PI-80	19.0	0.55	5.7	1.6	4.2
PI-140	33.3	0.48	5.4	1.6	4.2
PI-224	53.2	0.41	5.3	1.6	4.2
PI-314	75.0	0.48	5.1	1.6	4.2
PBO-100	11.1	0.36	3.1	1.1	8.9

Table 2 summarizes the fitting results obtained from modeling the viscoelastic polyisoprene data.

Next, we kept the value for τ_e fixed to the average value 1.62×10^{-5} s since it only depends on the specific chain properties and thus should be constant for polyisoprene. We then determined the entanglement number Z by fitting the normalized dielectric spectrum $\varepsilon''/\Delta\varepsilon$ directly to eq 8 (assuming no CR contribution). Additionally, we allowed the normalized relaxation strength $\Delta\varepsilon$ to be a free parameter to account for small errors in the normalization of the measured BDS curves. Finally, the viscoelastic data were refitted with these τ_e and Z while leaving c_ν and G_e free for minimization. The obtained plateau modulus G_e was used for the normalization of the curves displayed in Figure 2a.

As can be seen in Figure 2, our combined fitting procedure yields a remarkably good quantitative description of both experimental spectra over the full frequency range of the global chain relaxation by using the same molecular parameters Z and τ_e. It is important to note that independently of the molecular weight our proposed description naturally accounts not only for the differences in the spectral shape but also for the apparent shift between the longest dielectric and viscoelastic relaxation times. Consequently, within our approach based on the LM theory it is not necessary to assume an additional CR contribution to the dielectric spectrum.

In order to test our procedure further, we studied another type-A polymer, poly(butylene oxide) (PBO), which is chemically and structurally different in comparison to PI. The experimental data together with the result of the joint description are displayed in Figure 3 for one molecular weight. Again, we are able to get a very good common description (solid lines) of viscoelastic and dielectric spectra by the theory.

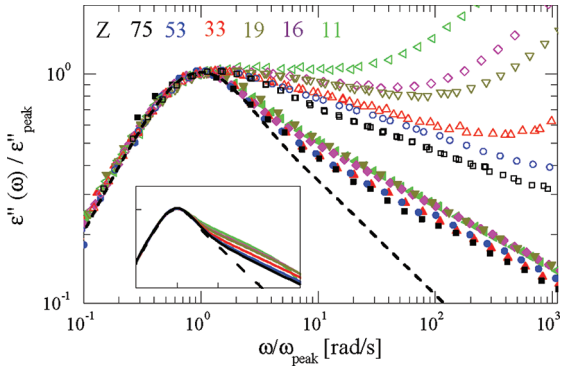

Figure 4. Plot showing the viscoelastic (unfilled symbols) and dielectric (filled symbols) loss parts normalized to the peak height and peak position. The dashed lines indicate the pure reptation prediction. The inset displays the normalized model predictions (eq 8).

The final parameters obtained from the joint fitting procedures are summarized in Table 3 for all samples.

DISCUSSION

Quantitative Description. Since the Likhtman−McLeish theory was developed for the description of mechanical stress relaxation, we will at first address the modeling of the viscoelastic data alone. Concerning the fit quality, the direct modeling by eq 7 (dashed orange lines in Figure 2a) as well as the joint description (solid lines) can equally well reproduce the experimental data. However, both procedures yield slightly different values for Z and c_ν in particular for the longer chains. The origin of the apparent discrepancy becomes evident by comparing the respective values (cf. Tables 2 and 3). Whereas increasing the number of entanglements Z shifts the peak to lower frequencies, higher values for c_ν effectively counteract by shifting it to higher frequencies as was shown in the theoretical part (inset of Figure 1). This behavior makes an accurate fitting rather intricate from viscoelastic data alone but the problem can be overcome by a joint fitting approach.

Assuming that the end-to-end vector relaxation is not affected by the constraint release motion (prerequisite for eq 8), the entanglement number Z can unequivocally be determined from the dielectric spectrum. In doing so, we obtain more consistent values for $M_e = 4.2 \pm 0.1$ kg/mol and less variations in $c_\nu = 0.45 \pm 0.1$ over the full range of molecular weights investigated. Considering the rather high scatter of the obtained values for the entanglement modulus G_e, the modulus relation $G_e = \rho RT/M_e$ is well fulfilled. In comparison to Auhl et al.,[30] our data yield a somewhat lower value for the entanglement molecular weight. Since in their work a fixed $c_\nu = 0.1$ is imposed, the obtained M_e = 4.8 kg/mol is of course expected to be higher for the same reason given just above (smaller $c_\nu \rightarrow$ smaller Z).

Our experimental results evidence that the solution given by the LM theory for the single chain relaxation function $\mu(t)$ is able to account for all the features of the dielectric normal mode relaxation, i.e., the peak position and peak shape, with a high degree of accuracy (cf. Figures 2b and 3). However, at high frequencies ($\omega > 10^4$ rad/s) a downward swing of the theory prediction appears in the dielectric spectrum. These deviations from the asymptotic power law behavior will be reasoned in the discussion of the relaxation mode distribution.

dx.doi.org/10.1021/ma200674z |*Macromolecules* 2011, 44, 7430–7437

Relaxation Mode Distribution. Based on a molecular theory, our description naturally provides a detailed molecular understanding of the peculiar narrow shape of the dielectric normal mode. The different features of the dielectric and viscoelastic relaxation mode spectra become most apparent when the loss parts are normalized to their peak height and peak position as displayed in Figure 4.

In direct comparison of dielectric (filled symbols) and viscoelastic (unfilled symbols) spectra, it is quite obvious that the dielectric mode distribution is much narrower and nearly identical for all molecular weights, in contrast to the viscoelastic mode distribution. The distinct kink resulting from the two power law behaviors at the high-frequency side of peak is well resolved in the dielectric spectra, whereas the viscoelastic spectra show only a single slope that is always smaller than $-1/4$.

Since we use in principle the same theory for the description of both spectra, we can easily explain these different features by comparing eq 7 with eq 8. In the viscoelastic spectrum the absence of the asymptotic $-1/4$ behavior is due to the longitudinal stress relaxation modes[4] which are obviously not seen in the dielectric experiment. Moreover, the fast local Rouse motion within the entanglement segments, introducing additional viscoelastic relaxation modes at very high frequencies, do not appear in the normal mode spectrum because the asymptotic behavior is preserved over several decades in frequency.

The observed downward swing of the theory function (lines in Figure 2b) for the lower molecular weight samples relates to the finite number of relaxation modes in the LM theory. Our experimental data do not display this behavior possibly because the loss at highest frequencies eventually increases due to the onset of the alpha-process, a separate relaxation process related to segmental correlations.[31] Such finite mode effects are experimentally observed for low molecular weight samples if the contribution of the alpha-process is subtracted.[14,32]

The absence of the CR term $R(t,c_\nu)$ in eq 8 is the only decisive difference to eq 7 and therefore evidence that the dielectric mode distribution is fully determined by the reptation and CLF motion alone. Consequently, the spectral shape of the end-to-end vector relaxation is insensitive to the CR motion, thus preserving the observed slope of $-1/2$ (reptation prediction, dashed lined) preceding the asymptotic behavior.

This result is in perfect harmony with various experiments on blends of dilute PI probes in PI or PB (polybutadiene) matrices of high and low molecular weight.[1,9,12,17−20] In particular, in blends where the CR contribution to the chain relaxation was physically suppressed by a high-M matrix the coincidence of the viscoelastic $\mu(t)$ and dielectric $\phi(t)$ relaxation functions was directly observed, and the viscoelastic relaxation mode distribution shows the same features as in the dielectric experiment.[9,20] Furthermore, the eigenmode analysis of Watanabe[1,19] on dipole-inverted chains clearly revealed nonsinusoidal eigenfunctions which were suspected to originate from additional relaxation mechanisms near the chain ends[1,10] and thus agree qualitatively with our CLF description.

Moreover, in blends where the long but dilute probe chains are not entangled among themselves, our findings can well explain the observed broadening of the loss curves in matrices with increasing M.[1,12,18] In the low-M matrices ($M < M_e$) the nonentangled probe chains obviously relax with the narrow mode distribution of a Rouse chain.[12,14,32] On the contrary, the dilute probe in the high-M matrix is yet again subject to the confining tube which is formed by the entangling matrix chains, resulting in the similarly broad

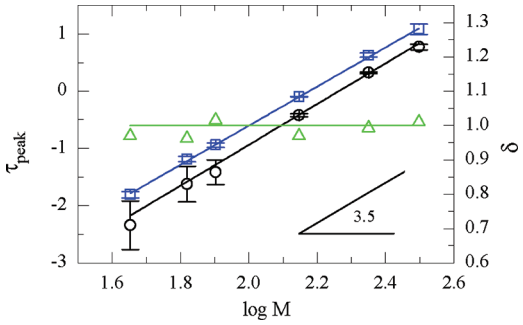

Figure 5. (left) Longest viscoelastic (circles) and dielectric (squares) relaxation times were extracted from the peak positions ($\tau_m = 1/\omega_{peak}$) and plotted vs M. (right) Scaling parameter δ (triangles) varies unsystematically around 1 for all M, indicating that the dielectric peak position is not accelerated by CR.

dielectric mode distribution (due to the CLF) as observed for the entangled homopolymer melts.[1,12]

***M*-Dependence of the Mode Spectrum.** Here, a remark concerning the M-dependence of the dielectric mode distribution needs to be made since there are contradictory findings reported in the literature.[1,8,13−15] The earlier dielectric data shown by Watanabe et al.[1,8] indicated that the slow dielectric mode distribution is insensitive to M over a broad range of molecular weights. However, a detailed inspection of our data encompassing even higher molecular weights as in the earlier study present small but systematic changes with M (Figure 4). These deviations manifest themselves in the gradually emerging second power law ($\omega^{-1/2}$) at low frequencies that relates to pure reptation and become more pronounced with increasing molecular weight. The otherwise observed $\omega^{-1/4}$ power law is quantitatively described by the CLF mechanism.

This slight M-dependence in the spectra of these well-entangled chains originates from the separation of pure reptation to CLF governed modes (cf. early and late time part in eq 5) as can be seen in Figure 4. Since CLF is only effective up to the Rouse time,[4] the deviations from the M-independent reptation dominated behavior decrease approximately with Z. The effect is clearly demonstrated in the inset of Figure 4 where the theory predictions are plotted as lines. These findings agree perfectly with the recently published results of Riedel et al.,[15] Abou Elfadl et al.,[14] and some earlier works.[7,16]

Competition between Reptation and CR. Our experimental findings suggest the intriguing conclusion that the thermal CR motion does not contribute to the dielectric chain relaxation at all, in contrast to the viscoelastic case. The absence of the CR process in the normal mode spectrum of course raises the question on how the competition between reptation with contour length fluctuation and the constraint release mechanism occurs in the dielectric end-to-end vector relaxation.

From a theoretical point of view, the rigorous formulation for this competition by the Watanabe−Tirrel model[33] in terms of a configuration-dependent constraint-release (CDCR) mechanism could well explain our experimental findings. The CDCR model clearly points out the differences in the correlation functions $S(n,t)$ and $C(n,t,n')$, resulting in different sensitivities with respect to the constraint release motion. Its theoretical prediction that the CR contribution is not reflected in the dielectric spectra is fully consistent with our experimental observation. However, the model is only valid for the case of pure reptation competing with the Rouse-like thermal CR. Nonetheless, it should at least approximately hold for describing the slowest dielectric

relaxation mode for which the LM theory assumes a pure reptation spectrum.

The model further predicts an acceleration of the longest dielectric relaxation time τ_ε by the CR motion if the respective time scales of reptation and CR relaxation are not too far apart: $\tau_\varepsilon = [\tau_{df}^{-1} + \tau_{CR}^{-1}]^{-1}$.[8] The ratio of the constraint release and reptation time was experimentally extrapolated for PI by Sawada et al.[34] from viscoelastic PI/PI blend data. In the case of only a few entanglements ($Z < 20$) their findings ($\tau_{CR} \approx 10\tau_{df}$) would thus predict a small shift of the observed dielectric relaxation time by about 10−20% at least for our low molecular weight samples. From the joint description of our dielectric and viscoelastic data in terms of the LM theory we conclude that no additional shift of the dielectric peak positions caused by CR is visible. This finding is further supported by fitting the dielectric data to a slightly modified version of eq 8 where an additional free scaling parameter $\delta\tau_{df}(Z)$ was introduced to allow an arbitrary shift of the longest relaxation time. However, the obtained fitting values for δ (green triangles in Figure 5) varied unsystematically around 1 for all molecular weights which indicates no sign of an additional peak shift by CR.

In Figure 5, the viscoelastic and dielectric terminal relaxation times $\tau_m = 1/\omega_{peak}$ were extracted from the peak positions and plotted vs the molecular weight. Our experimental data evidence that both terminal times have the same M-scaling with the typical power law $M^{3.5\pm0.1}$ which clearly deviates from the pure reptation prediction.[1,4,12,14] Note that the LM theory predicts that the viscosity η, which scales in the same fashion as τ_m, has a constraint release (c_ν) independent M-scaling dependence where only the absolute values depend on the actual amount of CR in the system.[4]

Our experimental findings well reflect the LM prediction but contradicts somewhat the experiments of Adachi et al.[12] on compatible PI/PB blends and of Liu et al. using probe rheology.[35] Adachi reported that CLF effects alone can be ruled out as the origin of the deviations from pure reptation since the $M^{3.0}$ dependence was observed for blends using a high-M matrix. Our results from dielectric experiments on homopolymer melts however clearly show that the CLF mechanisms would fully account for the deviation.

We would like to stimulate further experimental and in particular theoretical work in order to verify our proposed model and to enhance the understanding on the competition of reptation with contour length fluctuations and the constraint release mechanisms. For instance, rigorously and carefully combined dielectric and viscoelastic experiments on PI/PI blends are necessary to investigate and separate the influence of CLF and CR on the terminal relaxation time by physically tuning the CR mechanism.

SUMMARY

In summary, we have performed dielectric and rheological studies of two type-A polymer melts. The experimental observations are summarized as follows: The viscoelastic spectra are perfectly described in terms of the Likhtman−McLeish theory. We demonstrated that the same single chain solution $\mu(t)$ can also fully describe all the features of the dielectric normal mode relaxation. In particular, we were able to use one common parameter set Z and τ_e per molecular weight to describe the shape as well as the peak frequency of the viscoelastic and dielectric data.

In agreement with recent reports from the literature, we clearly showed that the dielectric mode spectrum depends slightly on the molecular weight as is predicted by the self-consistent treatment of CLF in the Likhtman−McLeish theory.

The comparison of our proposed dielectric relaxation function with the experimental data evidenced that its spectral shape is completely determined by reptation and CLF motion, thus unaffected by a CR contribution. We found that even the terminal dielectric relaxation time is not shifted by the CR process within the experimental accuracy. Since the dielectric method is insensitive to the CR process, it allows the direct observation of the pure single-chain dynamics. Hence, an accurate characterization of reptation and CLF is possible.

In the future further experiments and theoretical work are necessary in order to test the applicability and limitations of our proposed model. The competition between reptation including contour length fluctuations and the CR mechanism can only unequivocally be investigated by appropriate PI/PI blends in which the strength of the constraint release contribution can systematically be tuned.

AUTHOR INFORMATION

Corresponding Author

*E-mail: g.j.schneider@fz-juelich.de.

ACKNOWLEDGMENT

The authors thank Dr. Lutz Willner for the synthesis of some of the polyisoprene samples. We gratefully acknowledge the funding by the Deutsche Kautschuk Gesellschaft, Frankfurt, Germany.

REFERENCES

(1) Watanabe, H. *Macromol. Rapid Commun.* **2001**, *22*, 127–175.
(2) De Gennes, P. G. *J. Chem. Phys.* **1971**, *55*, 572–579.
(3) Doi, M.; Edwards, S. F. *The Theory of Polymer Dynamics; International Series of Monographs on Physics*; Oxford University Press: Oxford, 1986 (reprinted 2007); Vol. 73.
(4) Likhtman, A. E.; McLeish, T. C. B. *Macromolecules* **2002**, *35*, 6332–6343.
(5) Wischnewski, A.; Monkenbusch, M.; Willner, L.; Richter, D.; Likhtman, A.; McLeish, T. C.; Farago, B. *Phys. Rev. Lett.* **2002**, *88*, 058301.
(6) Adachi, K.; Yoshida, H.; Fukui, F.; Kotaka, T. *Macromolecules* **1990**, *23*, 3138.
(7) Roland, C. M.; Bero, C. A. *Macromolecules* **1996**, *29*, 7521–7526.
(8) Watanabe, H. *Prog. Polym. Sci.* **1999**, *24*, 1253–1403.
(9) Matsumiya, Y.; Watanabe, H.; Osaki, K. *Macromolecules* **2000**, *33*, 499–506.
(10) Watanabe, H. *Polym. J.* **2009**, *41*, 929–950.
(11) Imanishi, Y.; Adachi, K.; Kotaka, T. *J. Chem. Phys.* **1988**, *89*, 7585–7592.
(12) Adachi, K.; Wada, T.; Kawamoto, T.; Kotaka, T. *Macromolecules* **1995**, *28*, 3588–3596.
(13) Hyun, K.; Hoefl, S.; Kahle, S.; Wilhelm, M. *J. Non-Newtonian Fluid Mech.* **2009**, *160*, 93–103.
(14) Abou Elfadl, A.; Kahlau, R.; Herrmann, A.; Novikov, V. N.; Rössler, E. A. *Macromolecules* **2010**, *43*, 3340–3351.
(15) Riedel, C.; Alegría, A.; Tordjeman, P.; Colemenero, J. *Rheol. Acta* **2010**, *49*, 507–512.
(16) Adachi, K.; Kotaka, T. *Prog. Polym. Sci.* **1993**, *18*, 585–622.
(17) Adachi, K.; Itho, S.; Nishi, I. *Macromolecules* **1990**, *23*, 2554–2559.
(18) Watanabe, H.; Urakawa, O.; Yamada, H. *Macromolecules* **1996**, *29*, 755–763.

(19) Matsumiya, Y.; Watanabe, H.; Osaki, K.; Yao, M. *Macromolecules* **1998**, *31*, 7528–7537.
(20) Watanabe, H.; Matsumiya, Y.; Osaki, K.; Yao, M. *Macromolecules* **1998**, *31*, 7538–7545.
(21) Ferry, J. D. *Viscoelastic Properties of Polymers*, 3rd ed.; John Wiley & Sons, Inc.: New York, 1980.
(22) Stockmayer, W. H. *Pure Appl. Chem.* **1967**, *15*, 539–554.
(23) Rubinstein, M.; Colby, R. H. *J. Chem. Phys.* **1988**, *89*, 5291–5306.
(24) Liu, C. Y.; Keunings, L.; Bailly, C. *Macromolecules* **2007**, *40*, 2946–2954.
(25) Abdel-Goad, M.; Pyckhout-Hintzen, W.; Kahle, S.; Allgaier, J.; Richter, D.; Fetters, L. J. *Macromolecules* **2004**, *37*, 8135–8144.
(26) Allgaier, J.; Willbold, S.; Chang, T. *Macromolecules* **2007**, *40*, 518–525.
(27) Williams, M. L.; Landel, R. F.; Ferry, J. D. *J. Am. Chem. Soc.* **1955**, *77*, 3701.
(28) Ramirez, J.; Likhtman, A. E. Rheology of Entangled Polymers: Toolkit for Analysis of Theory & Experiment. http://www.reptate.com/, Version 1.0 (April 14, 2009).
(29) Galassi, M. *GNU Scientific Library Reference Manual*, 3rd ed.); ISBN 0954612078: http://www.gnu.org/software/gsl/.
(30) Auhl, D.; Ramirez, J.; Likhtman, A. E.; Chambon, P.; Fernyhough, C. *J. Rheol.* **2008**, *52*, 801–835.
(31) Kremer, F.; Schönhals, A. *Broadband Dielectric Spectroscopy*; Springer-Verlag: Berlin, 2003.
(32) Riedel, C.; Alegría, A.; Tordjeman, P.; Colmenero, J. *Macromolecules* **2009**, *42*, 8492–8499.
(33) Watanabe, H.; Tirrel, M. *Macromolecules* **1989**, *22*, 927–939.
(34) Sawada, T.; Qiao, X.; Watanabe, H. *Nihon Reoroji Gakkaishi* **2007**, *35*, 11–20.
(35) Liu, C.-Y.; Keunings, R.; Bailly, C. *Phys. Rev. Lett.* **2006**, *97*, 246001.